Granular Matter (2011) 13:487–492
DOI 10.1007/s10035-011-0260-9

ORIGINAL PAPER

Accuracy of the toroidal approximation for the calculus of concave and convex liquid bridges between particles

David Megias-Alguacil · Ludwig J. Gauckler

Received: 28 September 2010 / Published online: 29 March 2011

Abstract In situations and processes where finely divided solids are in contact with small amounts of liquid, capillary effects influence the behavior of such systems. If the quantity of liquid is rather limited, it arranges as individual liquid bridges connecting the solid particles just wetting a portion of the solids surface. These bridges develop forces which drive the cohesion and motion of the solid particles, further determining in many times the final structure or even the quality of the material. Since the liquid is not able to fully cover the solid particles like in a proper suspension, this liquid adopts a shape which is determined by the principle of constant mean curvature. A rigorous determination of such a shape, which in turn determines the capillary forces, must be carried out by solving the Young–Laplace equation. Due to the difficulties in such calculation, it was proposed to approximate the meniscus profile by an arc-of-circumference, the so-called toroidal approximation. Here it is quantitatively studied the suitability of such approximation for the most general geometry of liquid bridges, finding that the error of the approximation is below 10% for concave menisci and 30% for convex ones.

Keywords Liquid bridges · Toroidal approximation · Meniscus · Young–Laplace equation

1 Introduction

Liquid bridges are a particular case of multi-phase systems, appearing when solid particles are joined together by small amounts of a liquid, insufficient to cover completely the solid surfaces. The liquid phase in this so-called pendular state is discontinuous. This scenario is found in many practical situations and processes involving growth of wet agglomerates and binder granulation [1–4], flotation systems [5], moist soils [6,7], inter-particle cohesion of wet granular media [8–12], liquid phase sintering [13–19], etc. The liquid is entrapped between the solid particles, thus inducing the onset of capillary forces which drives the system to shrink or to expand according to the attractive or repulsive nature of the resulting force. This behavior is of importance when e.g. it may provoke structural defects hindering the quality of a material. The determination of such capillary forces has been the focus of a complete body of research, e.g. [14,20–28]. Essentially, the capillary forces depend upon the geometry of the liquid meniscus: curvature and three-phase-contact line length; and in turn, this geometry mainly depends on three variables: wetting angle, inter-particle separation and liquid amount of the bridge.

D. Megias-Alguacil (✉) · L. J. Gauckler
Department of Materials, Non-Metallic Inorganic Materials,
ETH-Zürich, 8093 Zürich, Switzerland
e-mail: david.megias@mat.ethz.ch

2 The Young–Laplace solution

The profile shape of the liquid meniscus, assuming absence of gravity or other buoyancy forces, must posses a constant pressure [29] and the meniscus the form of a surface of revolution [30,31] with the same mean curvature everywhere [25,32], satisfying the Young–Laplace equation, which reads:

$$\frac{\Delta P}{\gamma} = \frac{1}{y(x)\left[1+y'(x)^2\right]^{1/2}} \pm \frac{y''(x)}{\left[1+y'(x)^2\right]^{3/2}} \qquad (1)$$

where γ is the surface tension of the liquid-gas interface, $y(x)$ is the function describing the liquid profile and $y'(x)$ and $y''(x)$ are its first and second derivative, respectively. The negative sign refers to a concave meniscus, meanwhile the

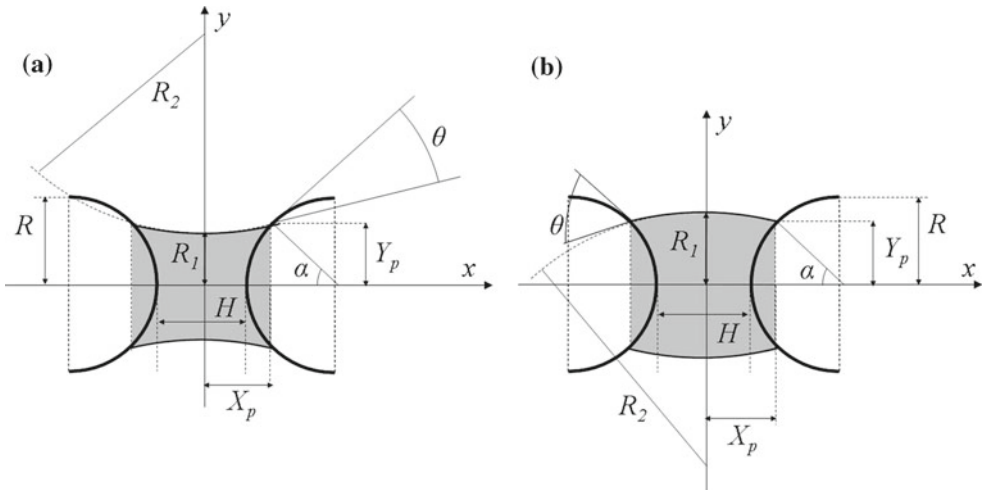

Fig. 1 Sketches of menisci with concave (**a**) and convex (**b**) geometries, displaying the parameters of interest

positive sign corresponds to a convex one. The capillary pressure, ΔP, is the pressure difference between the inner (liquid) and outer (gas) phases, $\Delta P = P_{inside} - P_{outside}$. This pressure difference may be described in terms of two principal radii of curvature, R_1 and R_2, of the meniscus (Fig. 1):

$$\Delta P = \gamma \left(\frac{1}{R_1} + \frac{1}{R_2} \right) \tag{2}$$

The radii can have positive or negative sign. Here, the sign convention will be positive if the radius lies inside the meniscus and negative when lying outside.

The resolution of Eq. 1 is rather complex and must be carried out by numerical computational methods. In addition, it is quite complicate to adjust *a priori* desired values of interest for the governing parameters: inter-particles distance, H, wetting angle, θ, and bridge liquid volume, V. Therefore, the determination of pressure differences at constant H, θ or V becomes a tedious task.

Another inconvenience which arises when solving exactly Eq. 1 is that the pressure difference is a parameter to be chosen before solving, but it may happen that several combinations of radii of curvature, Eq. 2, give the same numerical value of ΔP. Thus, the resolution of the equation may fall in a certain sort of ambiguity. Also, the solution of the Young–Laplace equation depends on the boundary conditions [25,27,33], and then the arising question is which solution is the correct one. This fact is of critical importance in the case of a possible coexistence of concave and convex menisci, because the simple value of ΔP is not enough to determine which geometry corresponds to the particular situation: neither the inter-particle distance neither the volume of the liquid in the inter-particle gap is taken into account at the time of solving Eq. 1. Thus, other aspects beyond the mathematics of the problem, like the energy of the bridge [27], must be considered in order to eliminate the ambiguity of the solution. This is why most probably, convex menisci have been many times neglected in case of possible coexistence, since they posses higher energy than concave ones.

3 The toroidal approximation

The so-called toroidal approximation, firstly proposed by Fischer [20], has been extensively used because it offers a much easier way of determining the shape of the liquid bridge, since this is assumed to be an arc-of-circumference, whose rotation around the symmetry axis determines the liquid surface. Figure 1 sketches such a geometry for both concave (Fig. 1a) and convex (Fig. 1b) cases, being R the solid particle's radius, X_p and Y_p are the abscissa and ordinate of the contact point between the solid and liquid profile, respectively; α is the half-filling angle, θ is the wetting angle determined from the tangents to the solid and liquid surfaces at the three-phase-contact point; R_1 and R_2 are the principal radii of curvature of the liquid meniscus, Eq. 2, measured orthogonally; H is the surface-to-surface distance between the solid particles. The reference system is chosen such that it origin is the middle point between the particles and whose x-axis lies along the straight line which joins the particles' centers. It is more convenient to use normalized quantities, therefore in what it follows, all lengths will be considered dimensionless by division by the particle radius R. Thus, the principal radii will be $r_1 = R_1/R$ and $r_2 = R_2/R$; the coordinate of the contact point $x_p = X_p/R$, $y_p = Y_p/R$; and the separation between particles $h = H/R$. The liquid volume of the bridge, V, will be also normalized to the volume of the spherical particle as $V_{rel} = V/V_{sphere}$.

The liquid profile can be written, using dimensionless coordinates x and y, under this approximation as:

$$y(x) = (r_1 \pm r_2) \mp \sqrt{r_2^2 - x^2} \tag{3}$$

where the upper signs correspond to the concave situation whereas the bottom signs to the convex case. The azimuthal radius r_1 is positive in both concave and convex cases, but the meridional radius, r_2, changes. It is negative in concave meniscus but positive in convex ones.

The radii r_1 and r_2 may be determined by calculating the volume of the liquid bridge, V_{rel}, for a giving set of inter-particles distance, h, and wetting angle, θ, values. They can be expressed as:

$$r_1 = y_p + r_2 \left[1 - \sin(\alpha + \theta)\right] \tag{4}$$

and

$$r_2 = \pm \frac{1 + h/2 - \cos\alpha}{\cos(\alpha + \theta)} \tag{5}$$

where the upper signs correspond to the concave situation whereas the bottom signs to the convex case, as above mentioned.

This volume determination can be carried out by definite integration:

$$V_{rel} = \frac{3}{2} \int_0^{x_p} [y(x)]^2 \, dx - \frac{3}{2} \int_{h/2}^{x_p} [y_S(x)]^2 \, dx \tag{6}$$

where x_p is the abscissa of the three-phase-contact point, $y(x)$ is given by Eq. 3, and $y_S(x) = \sqrt{1 - (x - h/2 - 1)^2}$ is the equation describing the solid particle contour, located at a distance h from the other particle.

Since when solving Eq. 6, the particular values of all the three parameters of interest: inter-particles distance, h, wetting angle, θ, and bridge liquid volume, V_{rel}, have to be selected before the corresponding calculation, the solution offered by the approximation is unique. Therefore, distinguishing concave from convex menisci is immediate and no further considerations are needed; moreover, concave-convex transitions, experimentally documented [34], are observed when varying the inter-particle distance.

Criticisms to the use of the toroidal approximation have been made on the basis that it is, obviously, an approximation to the exact solution, but previous works [16,25,30,33,35] show that this approximation bring a small error, <10%, respect to the exact solution of the Young–Laplace equation, Eq. 1. This error has been calculated and also measured [34] for the case of concave liquid bridges, but no information, to our best knowledge, is present in the literature for the convex bridges. In the present paper, the accuracy of the toroidal approximation will be evaluated for both geometries.

According to Hotta et al. [35], a function describing the liquid profile, $y(x)$, will be a solution of the Young–Laplace equation if it satisfies Eq. 1, in other case, there will be an error, ε. This error is a measure of the deviation of the approximation relative to the exact solution. Therefore, the error brought by the toroidal approximation can be evaluated if taking Eq. 3 into Eq. 1. Considering that the parameters involved in the calculations are normalized, the error ε is also dimensionless, and it may be expressed as:

$$\varepsilon(x) = \frac{1}{y(x)\left[1 + y'(x)^2\right]^{1/2}} \pm \frac{y''(x)}{\left[1 + y'(x)^2\right]^{3/2}} - \left(\frac{1}{r_1} \pm \frac{1}{r_2}\right) \tag{7}$$

This error depends on the local position, x, and therefore is more convenient to compute it along the whole liquid profile by means of the root mean squared error, E:

$$E = \left[\frac{1}{x_p} \int_0^{x_p} \varepsilon^2(x) dx\right]^{1/2} \tag{8}$$

where x_p is the abscissa of the three-phase-contact point. Notice that there are two situations in which the toroidal approximation is an exact solution: the case of cylindrical and spherical menisci ($r_1 = -r_2$), which are particular cases of geometries with constant curvature.

For a particular set of inter-particles distance, h, wetting angle, θ, and relative liquid volume, V_{rel}, values, the corresponding meniscus can be determined with the toroidal approximation by solving Eq. 6. This procedure implies determining the parameter x_p, and with this value, those of the principal radii, r_1 and r_2, Eqs. 4 and 5, taking into account the following geometrical relationships: $x_p = h/2 + (1 - \cos\alpha)$ and $y_p = \sin\alpha$, Fig. 1. Once obtained the radii, r_1 and r_2, recall defined at the meniscus neck, the equation of the liquid profile, $y(x)$, is then expressed by Eq. 3. This function is introduced into Eq. 7, giving thus the error $\varepsilon(x)$, from which the root mean squared error E, Eq. 8, of the meniscus calculated with the toroidal approximation is determined. The error brought by the toroidal approximation takes into account the differences of mean curvature respect to the exact solution.

4 Results

On next items, the error brought by the toroidal approximation will be calculated as a function of the depending parameters: h, θ and V_{rel}. Recall that all quantities involved in the ongoing calculations are normalized. The minimum and maximum distances h allowed for a particular liquid bridge depends upon the corresponding values of θ and V_{rel}; they can be found in detail elsewhere [36,37]. In addition, it will be considered that the solid particles are all spherical, equally sized and whose surfaces are perfectly smooth and

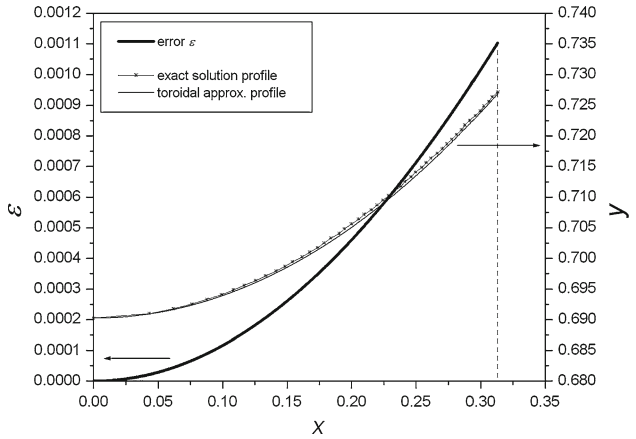

Fig. 2 Left axis: Error $\varepsilon(x)$, Eq. 7, as a function of the dimensionless coordinate, x, for a meniscus corresponding to $h = 0, \theta = 30°$ and $V_{rel} = 0.1$. Right axis: *solid* and *dotted lines* corresponding to the profiles $y(x)$ of this meniscus, obtained with the toroidal approximation and the exact solution, respectively. The *vertical dotted line* indicates the coordinate of the three-phase-contact-point, x_p (Fig. 1)

chemically homogeneous, not exhibiting any wetting hysteresis [38].

It has been mentioned above that the error, $\varepsilon(x)$, Eq. 7 varies along the profile of each particular meniscus. Figure 2 shows this behavior for the exemplary case of the meniscus which binds two particles at distance $h = 0$, with $\theta = 30°$ and $V_{rel} = 0.1$. The error, only displayed between $x = 0$ and $x = x_p$ (perpendicular dotted line) for the sake of clarity, is null when $x = 0$. Indeed, it is at the neck of the meniscus where the principal radii of curvature, r_1 and r_2, are defined in the approximation, Fig. 1, and thus, this is the only point where the approximation is essentially correct. Therefore, at the neck, both approximation and exact solutions coincide. As the local curvature is measured in another abscissa x along the liquid profile, a deviation respect to the exact solution is observed. The local error of the approximation, $\varepsilon(x)$, is higher as the measure is taken closer to the solid particles. This deviation is maximal at the three-phase-contact-point, $x = x_p$.

Also displayed in Fig. 2 are the profiles $y(x)$ of the corresponding liquid bridge meniscus determined through the toroidal approximation and the exact solution of the Young–Laplace equation, Eq. 1. Although both profiles look very similar in shape, the deviation brought by the approximation respect to the exact solution is noticeable in the plot. The difference between the profiles therefore induces a difference in the volume between both exact and approximated menisci. Indeed, since the curvature depends on the principal radii, the error in the curvature calculated with the toroidal approximation, Eq. 6, induces an error on the volume and other parameters involved. After checking the error in the volume, it is observed that this is of the same order than the error in the curvature.

4.1 Effect of wetting angle

Figure 3 shows the root mean squared error, E, as a function of the dimensionless inter-particle distance, h, when the relative liquid volume of the toroidal approximation $V_{rel} = 1$, for increasing wetting angles, θ.

As a general trend, it is observed that the error, E, increases when increasing the wetting angle, θ. Nevertheless, this error brought by the toroidal approximation is below 5% in all cases, despite that the menisci are highly convex for the higher values of θ.

Observe that in some cases, the error passes through 0 at a certain distance which corresponds to a cylindrical meniscus, transition case between the convex and concave geometries. A cylinder is a particular case of topology with constant mean curvature; therefore it fulfills the Young–Laplace equation, showing no error. At smaller distances, the liquid bridge is convex and concave for the largest separations between the particles. For these cases, the error decreases with the distance h as the convex meniscus approaches to the cylindrical shape, and increases as the concave bridge departs from that profile shape. In absolute value, considering all the range of possible inter-particle distance, the concave menisci shows smaller error than the convex ones with same V_{rel} and θ, but their error decreases with the amount of liquid because the shape tends to be more cylindrical as the inter-particles gap is filled.

In the rest of cases, when θ enlarges, the meniscus is convex at all possible distances, and E decreases monotonically

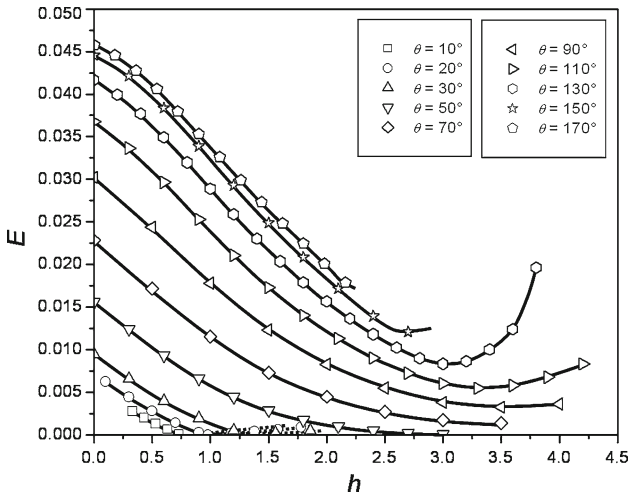

Fig. 3 Root mean squared error, E, Eq. 8, as a function of the dimensionless inter-particle distance, $h = H/R$, for liquid bridges of varying wetting angle, θ, when the volume of the toroidal approximation is $V_{rel} = 1$. *Solid lines* correspond to convex menisci and *dotted lines* to concave menisci

as the inter-particle separation, h, grows. For $\theta \geq 90°$, when allowed, there is a certain distance for which the trend of E is reversed, increasing with h. This is due to the decreasing of the height of the contact point between the liquid and the solid surfaces, y_p, when h enlarges much, provoking the bridge profile to increase its curvature at distances close to the particle surface, thus increasing the error E.

4.2 Effect of volume

Figures 4 and 5 show the mean square error, E, as a function of the inter-particle distance, h, for different toroidal approximation liquid volumes at $\theta = 30°$ and $\theta = 150°$, respectively. For volumes and wetting angles enabling the concave geometry, it is observed that E increases with h, but decreases with increasing the amounts of liquid, V_{rel}. On contrary, for the convex geometry, the error is maximal at the shortest distances, decreasing as the particles depart away.

As a general trend, the error E increases with V_{rel} for $\theta < 90°$, although remaining below 1%. In this case, as the liquid volume increases, the minimum possible distance between the particles is found at larger separations, where the error is smaller.

The error E decreases with V_{rel} when $\theta = 150°$ and more generally when $\theta > 90°$. The bridge liquid volume must be smaller than ∼10% for finding errors beyond 10% at the shortest separations between the particles, h. Calculations covering all values of wetting angle indicate that in any case, the error E tends to a maximum of ∼30% when $\theta > 90°$ and $V_{rel} \to 0$ for full contact between the particles, $h = 0$. Nevertheless these conditions must be considered as an unfeasible limit, since at vanishing liquid volumes it should not exist a proper liquid bridge and when the particles are very close, other interactions than the capillary, e.g. van der Waals forces, play a significant role [39].

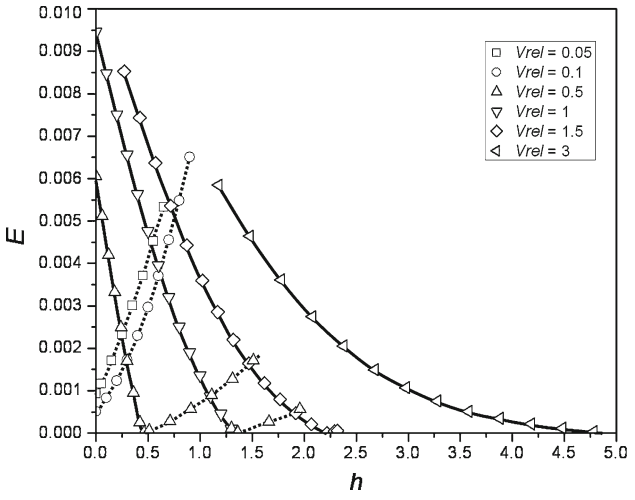

Fig. 4 Root mean squared error, E, Eq. 8, as a function of the dimensionless inter-particle distance, $h = H/R$, for liquid bridges of varying relative volume of the toroidal approximation, V_{rel}, when $\theta = 30°$. *Solid lines* correspond to convex menisci and *dotted lines* to concave menisci

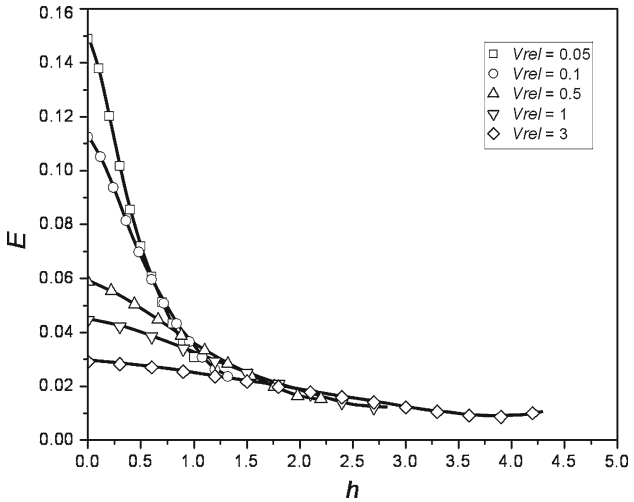

Fig. 5 Same than Fig. 4, but for $\theta = 150°$

The above discussion is valid for equally sized spheres. In case that the spheres have different sizes, the errors are likely to be larger. Indeed, if the spheres are not equal, the meniscus will not have its symmetry point aligned within the origin of the reference system, but displaced, thus being ε larger.

The error brought by the approximation when determining the curvature of the liquid bridge profile has an impact in the forces which arise between the solid particles. These capillary forces depend, beside the curvature of the meniscus, on experimental magnitudes like the size of the particles or the interfacial tension. The error in these forces will be, therefore, the combination of those errors associated to the determination of these magnitudes. If the particles size and interfacial tension can be experimentally determined with high accuracy, the force error would be then the error in curvature through its effect in the pressure difference, as discussed.

5 Conclusions

The error brought by the so-called toroidal approximation used for determining the shape of a liquid meniscus which bridges a pair of spherical particles can be easily determined by evaluating it on the Young–Laplace equation, for both concave and convex geometries. It is found that, for equally sized spheres, the maximum error remains below 10% when the bridge is concave, and ∼ 30% when the liquid bridge is convex.

The Young–Laplace equation was solved exactly for both concave and convex situations writing a program in the commercial software package Mathematica 7 following a similar scheme than in [27,40], finding profiles to particular

values of pressure and adjusting particular values of interparticle distances in order to obtain random combinations of wetting angle and liquid volume. The results of the comparison between the exact and approximated solutions were in excellent agreement with the results of the procedure here exposed. Therefore, it is shown the pertinence of using the approximation instead of solving the complex Young–Laplace equation, especially in experimental scenarios, where the magnitude of the experimental errors is comparable or higher to the error brought by the approximation. Alternatively, the method exposed here enables an easy determination of the error brought when employing the toroidal approximation in a particular situation.

References

1. Seville, J.P.K., Tuzun, U., Clift, R.: Processing of Particulate Solids. Kluwer, Dordrecht (1997)
2. Mort, P.R.: Scale-up of binder agglomeration processes. Powder Tech. **150**, 86–103 (2005)
3. Tardos, G.I., Khan, M.I., Mort, P.R.: Critical parameters and limiting conditions in binder granulation of fine powders. Powder Tech. **94**, 245–258 (1997)
4. Li, H.M., McCarthy, J.J.: Cohesive particle mixing and segregation under shear. Powder Technol. **164**, 58–64 (2006)
5. Kondrat'ev, S.A.: Influence of main flotation parameters on detachment of hydrophilic particle from bubble. J. Mining Sci. **41**, 373–379 (2005)
6. Haines, W.B.: Studies in the physical properties of soils. J. Agric. Sci. **15**, 529–543 (1925)
7. Molenkamp, F., Nazemi, A.H.: Interactions between two rough spheres, water bridge and water vapour. Geotechnique **53**, 255–264 (2003)
8. Groger, T., Tuzun, U., Heyes, D.M.: Modelling and measuring of cohesion in wet granular materials. Powder Technol. **133**, 203–215 (2003)
9. Pierrat, P., Caram, H.S.: Tensile strength of wet granular materials. Powder Technol. **91**, 83–93 (1997)
10. Lu, N., Wu, B.L., Tan, C.P.: Tensile strength characteristics of unsaturated sands. J. Geotech. Geoenviron. Eng. **133**, 144–154 (2007)
11. Richefeu, V., El Youssoufi, M.S., Radjai, F.: Shear strength properties of wet granular materials. Phys. Rev. E. **73**, 051304 (2006)
12. Kohonen, M.M., Geromichalos, D., Scheel, M., Schier, C., Herminghaus, S.: On capillary bridges in wet granular materials. Physica A. **339**, 7–15 (2004)
13. Kingery, W.D.: Densification during sintering in the presence of a liquid phase. J. Appl. Phys. **30**, 301–306 (1959)
14. Heady, R.B., Cahn, J.W.: An analysis of capillary forces in liquid-phase sintering of spherical particles. Metall. Trans. **1**, 185–189 (1970)
15. Hu, C., Baker, T.N.: An analysis of the capillary force and optimum liquid volume in a transient liquid phase sintering process. Mat. Sci. Eng. A. **190**, 125–129 (1995)
16. Delannay, F., Pardoen, D., Colin, C.: Equilibrium distribution of liquid during liquid phase sintering of composition gradient materials. Acta Mat. **53**, 1655–1664 (2005)
17. Liu, J., Cardamone, A.L., German, R.M.: Estimation of capillary pressure in liquid phase sintering. Powder Met. **44**, 317–324 (2001)
18. Nikolic, Z.S.: A simple model for 3-D visualization of model topology due to rearrangement in liquid phase sintering. Comput. Math. Appl. **51**, 551–558 (2006)
19. Eremenko, V.N., Naidich, Y.V., Lavrinenko, I.A.: Liquid-Phase Sintering. Consultants Bureau, New York (1970)
20. Fischer, R.A.: On the capillary forces in an ideal soil: correction of the formulae given by W.B. Haines. J. Agric. Sci. **16**, 492–505 (1926)
21. Huppmann, W.J., Rieger, H.: Modelling of rearrangement processes in liquid phase sintering. Acta Met. **23**, 965–971 (1975)
22. Pietsch, W., Rumpf, H.: Haftkraft, Kapillardrudr, Fliissigkeitsvolumen und Grenzwinkel einer Fliissigkeitsbriicke zwischen zwei Kugeln. Chemie Ing. Techn. **39**, 885–893 (1967)
23. Chan, D.Y.C., Henry, J.D., White, L.R.: The interaction of colloidal particles collected at fluid interfaces. J. Colloid Interface Sci. **79**, 410–418 (1981)
24. Erle, M.A., Dyson, D.C., Morrow, N.R.: Liquid bridges between cylinders, in a torus, and between spheres. AIChE J. **17**, 115–121 (1971)
25. Orr, F.M., Scriven, L.E., Rivas, A.P.: Pendular rings between solids—meniscus properties and capillary force. J. Fluid Mech. **67**, 723–742 (1975)
26. Mehrotra, V.P., Sastry, K.V.S.: Pendular bond strength between unequal-sized spherical-particles. Powder Technol. **25**, 203–214 (1980)
27. De Bisschop, F.R.E., Rigole, W.J.L.: A physical model for liquid capillary bridges between adsorptive solid spheres- the nodoid of Plateau. J. Colloid Interface Sci. **88**, 117–128 (1982)
28. Bayramli, E., Abou-Obeid, A., van de Ven, T.G.M.: Liquid bridges between spheres in a gravitational field. J. Colloid Interface Sci. **116**, 490–502 (1987)
29. Meurisse, M.H., Querry, M.: Squeeze effects in a flat liquid bridge between parallel solid surfaces. J. Tribol. **128**, 575–584 (2006)
30. Mazzone, D.N., Tardos, G.I., Pfeffer, R.: The effect of gravity on the shape and strength of a liquid bridge between 2 spheres. J. Colloid Interface Sci. **113**, 544–556 (1986)
31. Dai, Z.F., Lu, S.C.: Liquid bridge rupture distance criterion between spheres. Int. J. Miner. Proc. **53**, 171–181 (1998)
32. Kralchevsky, P.A., Nagayama, K.: Particles at fluid interfaces and membranes. Elsevier, Amsterdam (2001)
33. Lian, G.P., Thornton, C., Adams, M.J.: A theoretical study of the liquid bridge forces between two rigid spherical bodies. J. Colloid Interface Sci. **161**, 138–147 (1993)
34. Pepin, X., Rossetti, D., Iveson, S.M., Simons, S.J.R.: Modeling the evolution and rupture of pendular liquid bridges in presence of large wetting hysteresis. J. Colloid Interface Sci. **232**, 289–297 (2000)
35. Hotta, K., Takeda, K. Iinoya K.: Capillary binding force of a liquid bridge. Powder Technol. **10**, 231–242 (1974)
36. Megias-Alguacil, D., Gauckler, L.J.: Capillary forces between two solid spheres linked by a concave liquid bridge: regions of existence and forces mapping. AIChE J. **55**, 1103–1109 (2009)
37. Megias-Alguacil, D., Gauckler, L.J.: Analysis of the capillary forces between two small solid spheres binded by a convex liquid bridge. Powder Technol. **198**, 211–218 (2010)
38. Willett, C.D., Adams, M.J., Johnson, S.A., Seville, J.P.K.: Capillary bridges between two spherical bodies. Langmuir. **16**, 9396–9405 (2000)
39. Megias-Alguacil, D., Gauckler, L.J.: Capillary and van der Waals forces between uncharged colloidal particles linked by a liquid bridge. Colloid Polym. Sci. **288**, 133–139 (2010)
40. Rynhart, P., McKibbin, R., McLachlan R., Jones, R.J.: Mathematical modeling of granulation: static and dynamic liquid bridges. Res. Lett. Inf. Math. Sci. **3**, 199–212 (2002)